Electronic Supplementary Information

Nitrogen- and iodine-doped microporous carbon derived from a hydrogen-bonded organic framework: an efficient metal-Free electrocatalyst for oxygen reduction reaction

Wen-Ju Liu,[a †] *Ya-Qiong Wen,*[b†] *Jia-Wei Wang,*[a] *Di-Chang Zhong,*[*,a,b] *Jing-Bo Tan*[a] *and Tong-Bu Lu*[*,a]

[a] Institute for New Energy Materials & Low Carbon Technologies, School of Material Science & Engineering, Tianjin University of Technology, Tianjin 300384, China

[b] School of Chemistry & Chemical Engineering, Gannan Normal University, Ganzhou 341000, China

E-mail: zhong_dichang@hotmail.com (D. C. Zhong);
lutongbu@mail.sysu.edu.cn (T. B. Lu)

Table S1. The yield of pyrolyzed carbon synthesized at different temperatures.

Carbon Materials	M(HOF-8)/mg	M(Carbon)/mg	Yield/%
C_{KI}	300	30	10.0
C_{700}	300	125	41.7
C_{800}	300	121	40.3
C_{900}	300	116	38.7
C_{1000}	300	100	33.3

Table S2. Content of elements in carbon materials calculated from XPS.

Carbon materials	C content/at%	O content/at%	N content/at%	Pyridinic N/at%	I content/at%
C_{KI}	82.97	8.89	7.42	1.97	0.71
C_{700}	84.99	10.23	4.78	1.22	0
C_{800}	83.39	12.20	4.42	1.16	0
C_{900}	80.95	15.27	3.78	1.09	0
C_{1000}	85.42	12.17	2.41	0.29	0

Table S3. BET surface areas and pore volumes of carbon materials.

Carbon materials	BET Surface Areas/m^2 g^{-1}	Total Pore Volumes/cm^3 g^{-1}
C_{KI}	1140	0.562
C_{700}	22	0.026
C_{800}	327	0.147
C_{900}	282	0.138
C_{1000}	142	0.078

Table S4. I_D/I_G values calculated from Raman spectra.

Carbon materials	I_D/I_G
C_{KI}	1.10
C_{700}	1.10
C_{800}	1.08
C_{900}	1.06
C_{1000}	1.05

Table S5. Various parameters of carbon materials for ORR catalysis obtained from RDE experiments.

Carbon materials	Onset potential/V *vs.* RHE	Halfwave potential/V *vs.* RHE	Limited current density (@0.213 V *vs.* RHE)/mA cm^{-2}	Kinetic current density (@0.830 V *vs.* RHE) /mA cm^{-2}
C_{KI}	0.944	0.828	4.96	4.470
C_{700}	0.744	0.539	2.02	0.004
C_{800}	0.862	0.705	3.64	0.112
C_{900}	0.850	0.704	2.76	0.077
C_{1000}	0.836	0.703	2.57	0.050
Pt/C	0.936	0.816	5.45	2.742

a) b)

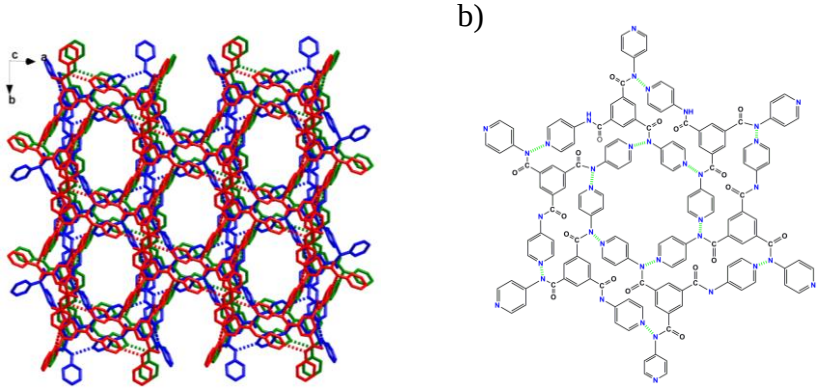

Fig. S1 a) The 3D supramolecular structure of HOF-8, and b) the chemical structure of HOF-8.

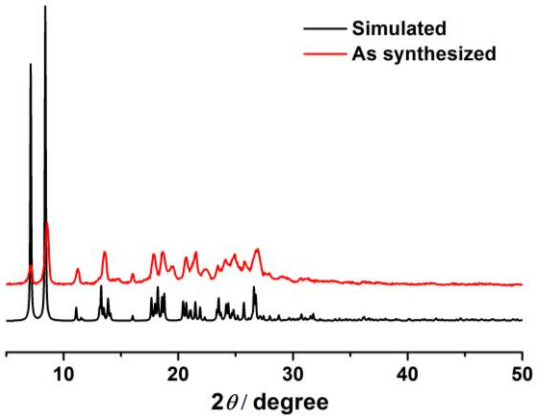

Fig. S2 Powder XRD of HOF-8 at room temperature.

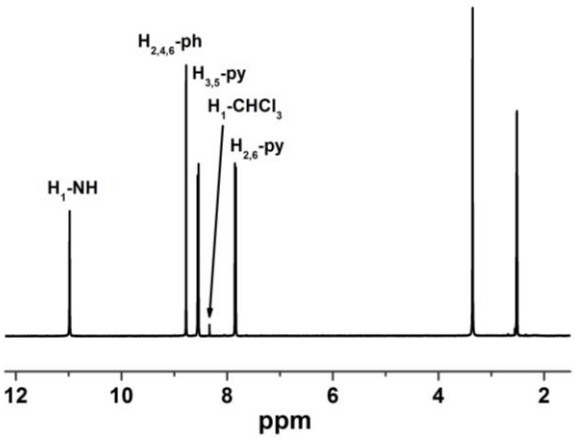

Fig. S3 ^{1}H NMR spectrum of HOF-8 (DMSO-d_6, 400 MHz, 298 K).

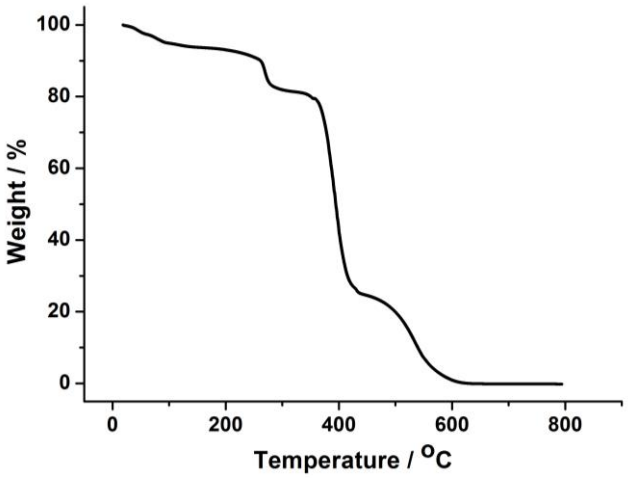

Fig. S4 TGA curve of HOF-8 at the N_2 atmosphere.

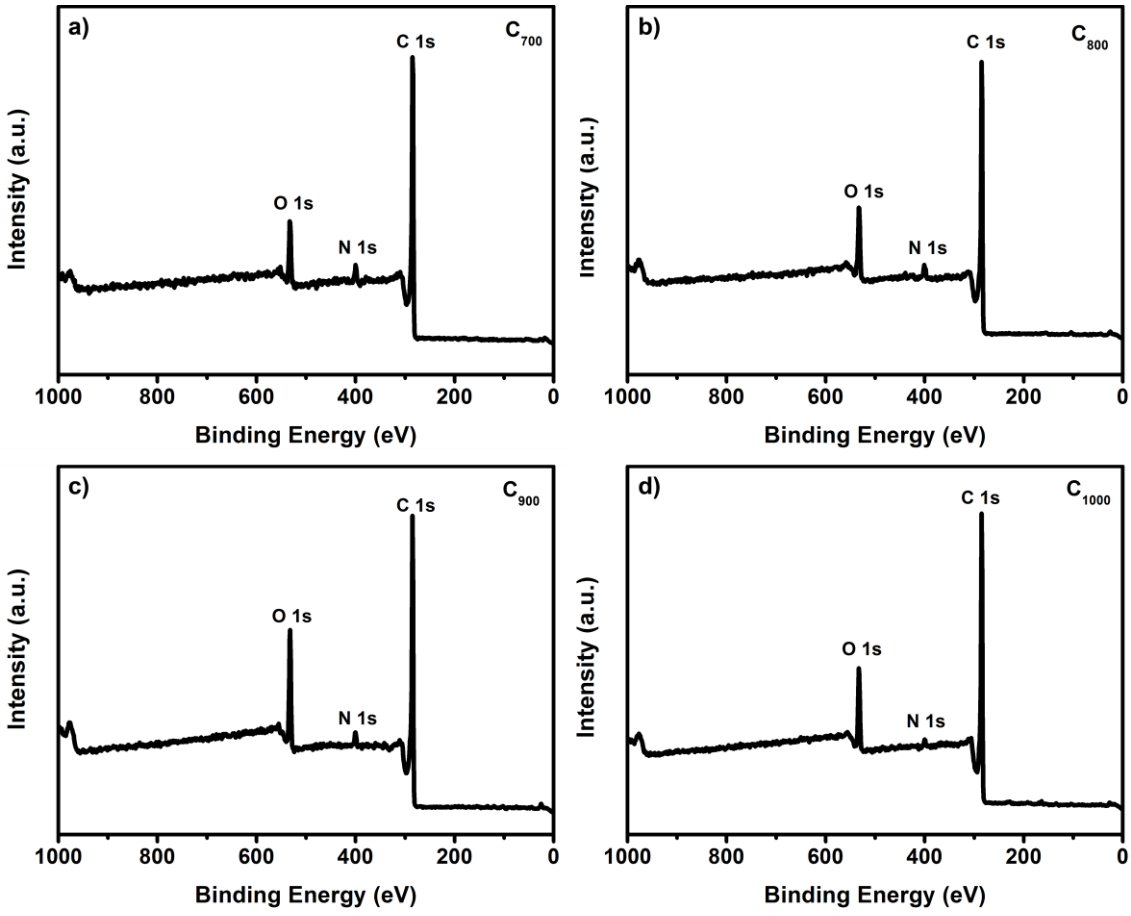

Fig. S5 XPS spectra of a) **C**$_{700}$, b) **C**$_{800}$, c) **C**$_{900}$ and d) **C**$_{1000}$.

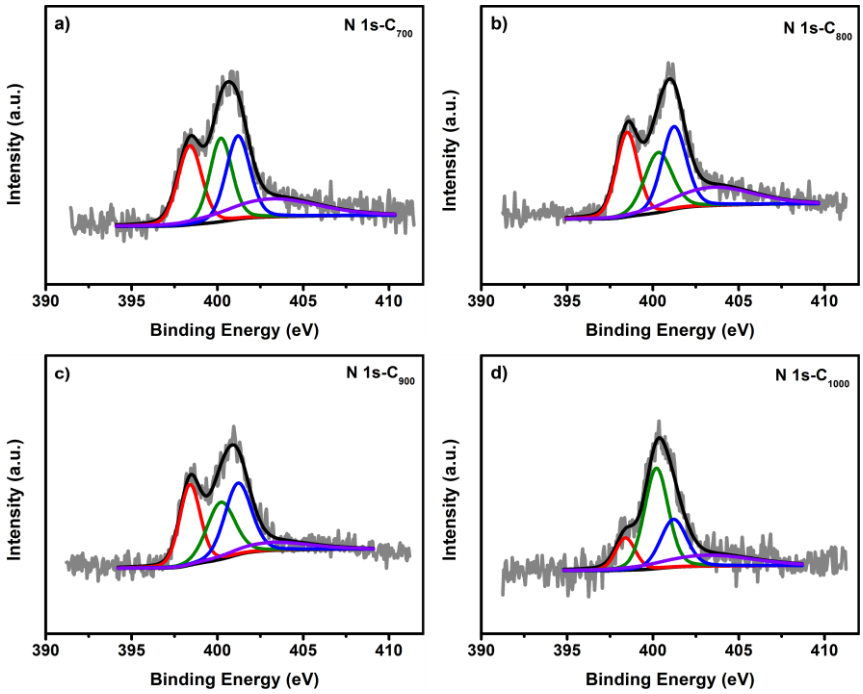

Fig. S6 High resolution N 1s spectra of a) **C700**, b) **C800**, c) **C900** and d) **C1000**.

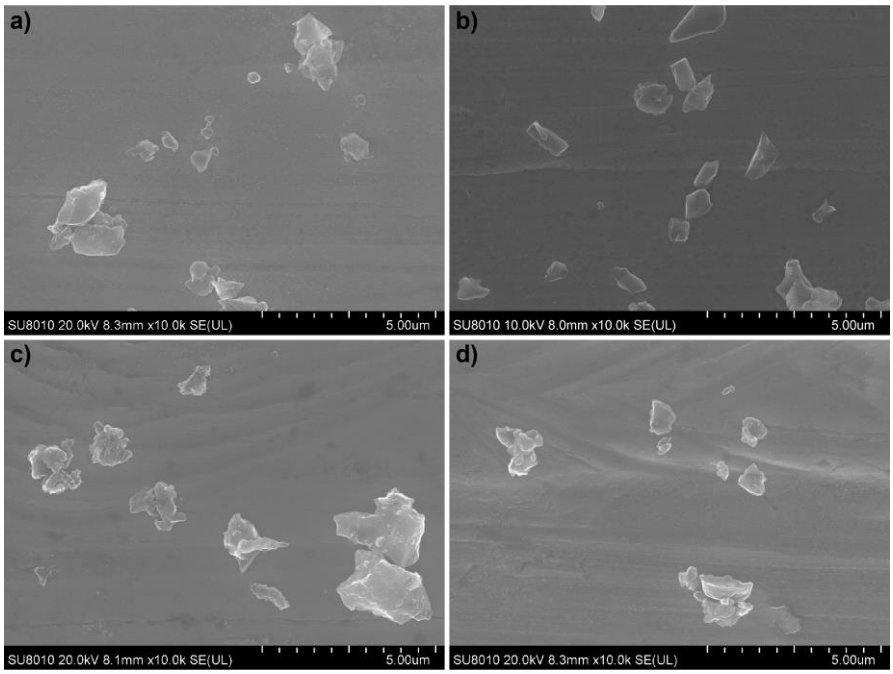

Fig. S7 SEM images of a) **C700**; b) **C800**; C) **C900**; d) **C1000**.

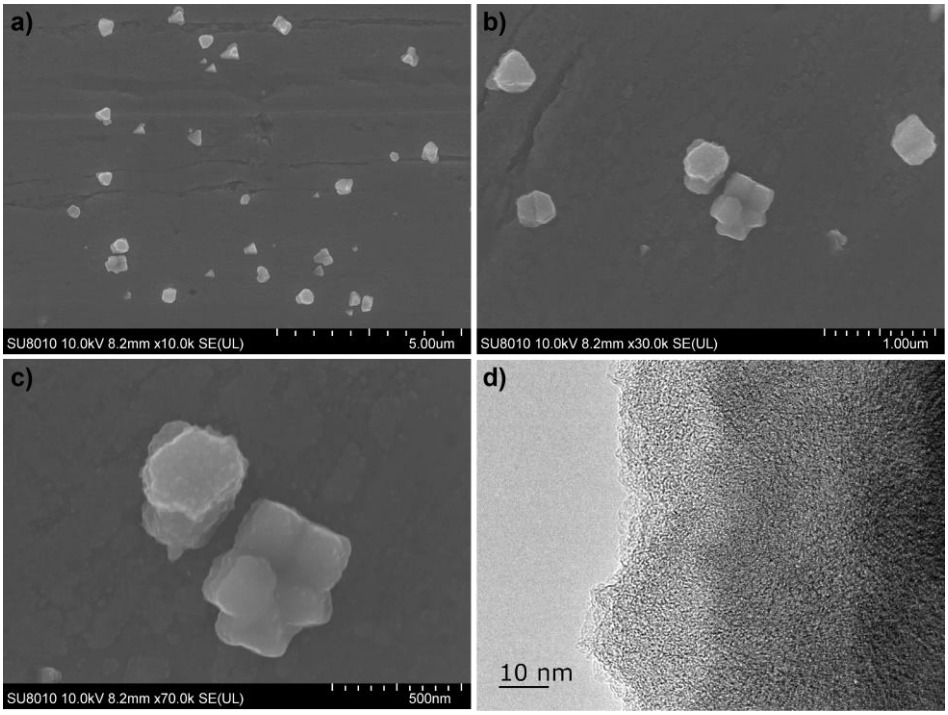

Fig. S8 a), b), c) SEM images showing the regular polyhedral shape and hierarchical structure of **C$_{KI}$**; d) TEM image of **C$_{KI}$**.

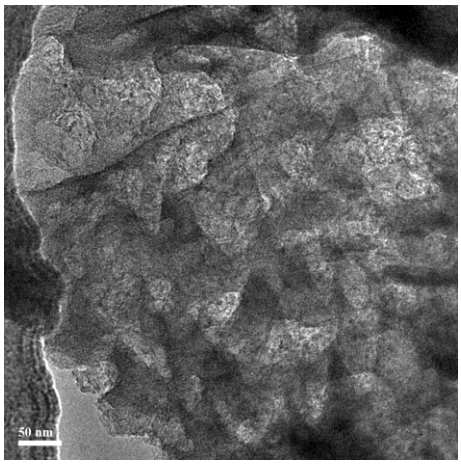

Fig. S9 TEM image of **C$_{KI}$**.

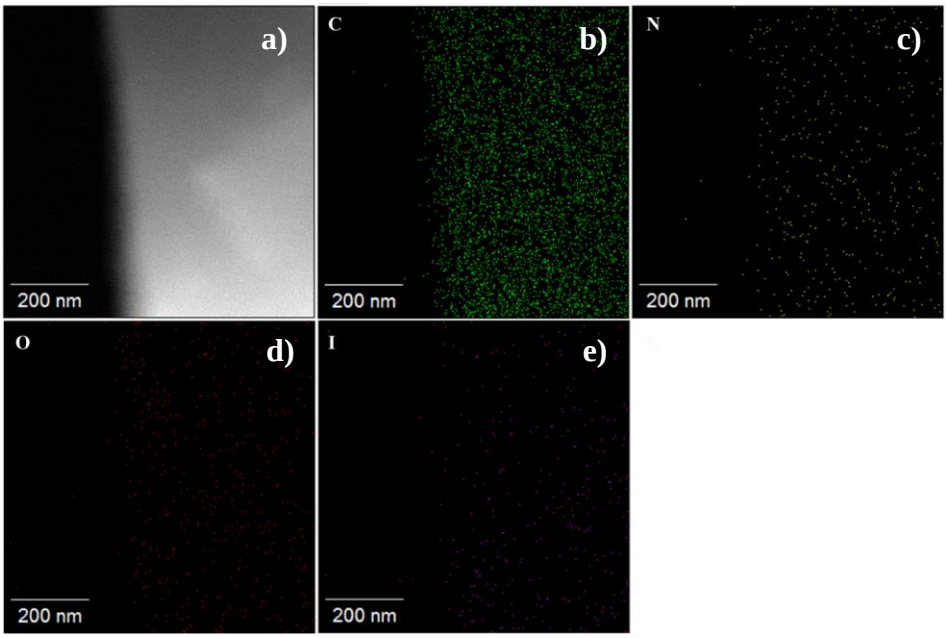

Fig. S10 a) TEM image of **C$_{KI}$** and the corresponding elemental mapping of b) C, c) N, d) O and e) I.

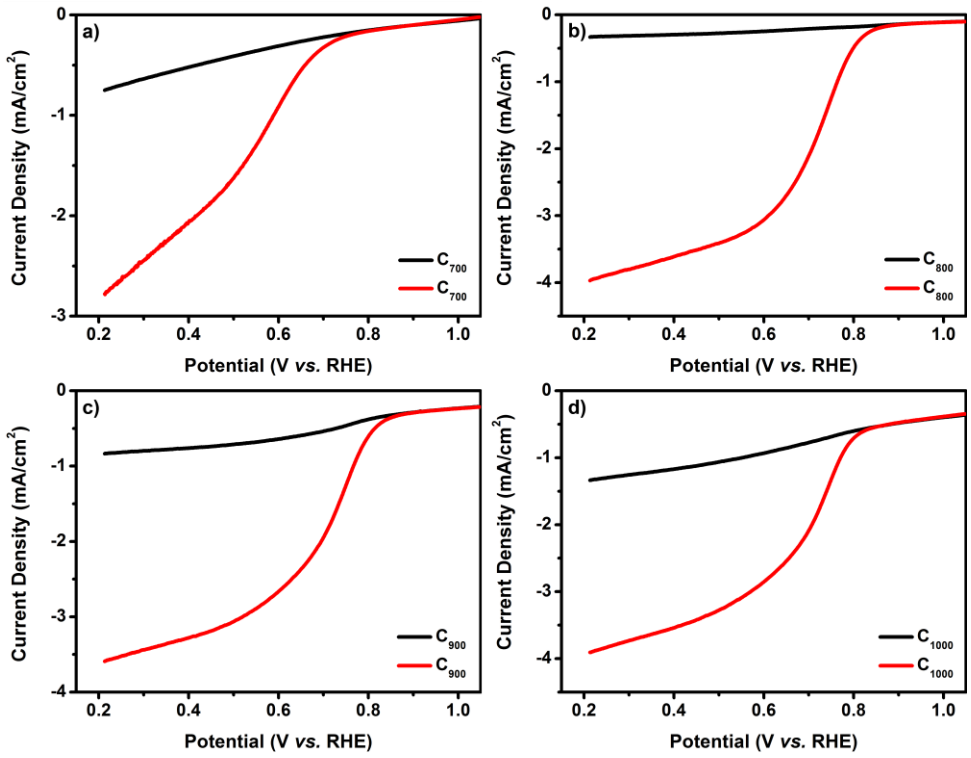

Fig. S11 RDE curves of a) **C$_{700}$**, b) **C$_{800}$**, C) **C$_{900}$** and d) **C$_{1000}$** in 0.1 M KOH solution saturated with N_2 (black) and O_2 (red).

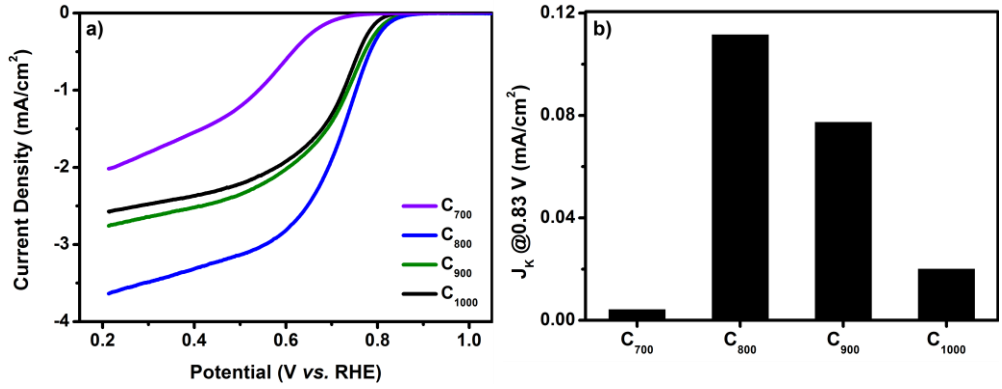

Fig. S12 a) LSV polarization curves of **C$_T$** at scanning speed of 10 mV s^{-1} and rotating speed of 1600 rpm in 0.1 M KOH solution with background subtraction. b) Comparison of kinetic current density of **C$_T$** at 0.83 V.

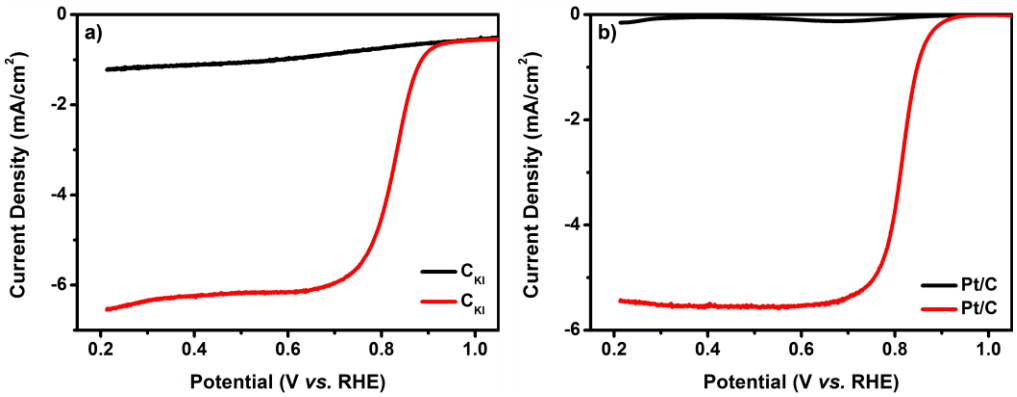

Fig. S13 RDE curves of a) **C$_{KI}$** and b) Pt/C in 0.1 M KOH solution saturated with N_2 (black) and O_2 (red).

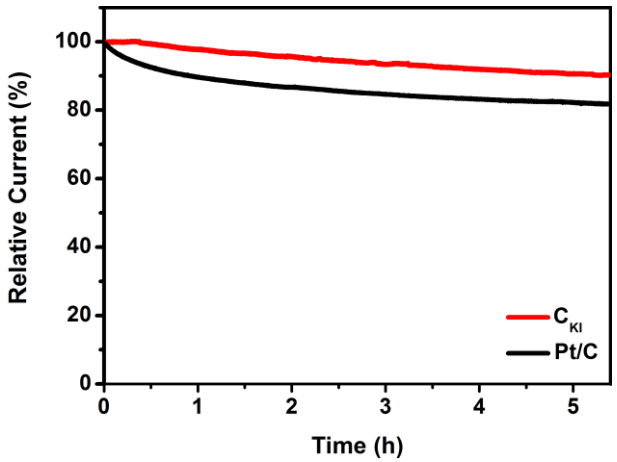

Fig. S14. Chronoamperometric responses of **C$_{KI}$** and 20 wt% Pt/C in O_2-saturated 0.1 M KOH at 0.764 V with 400 rpm rotating speed.

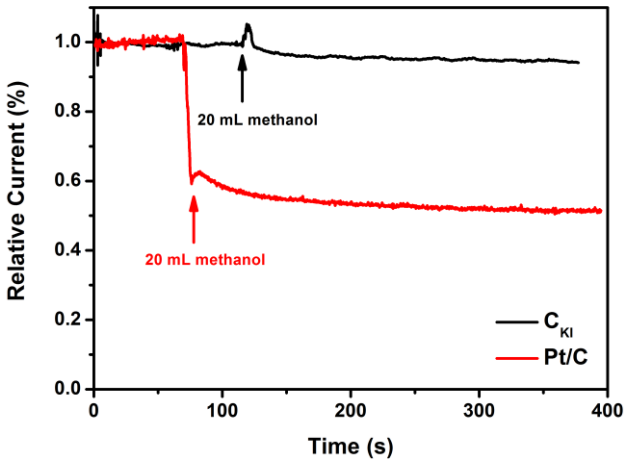

Fig. S15 Chronoamperometric responses of **C_{KI}** and 20 wt% Pt/C in O_2-saturated 0.1 M KOH under methanol addition at 0.764 V with 400 rpm rotating speed.

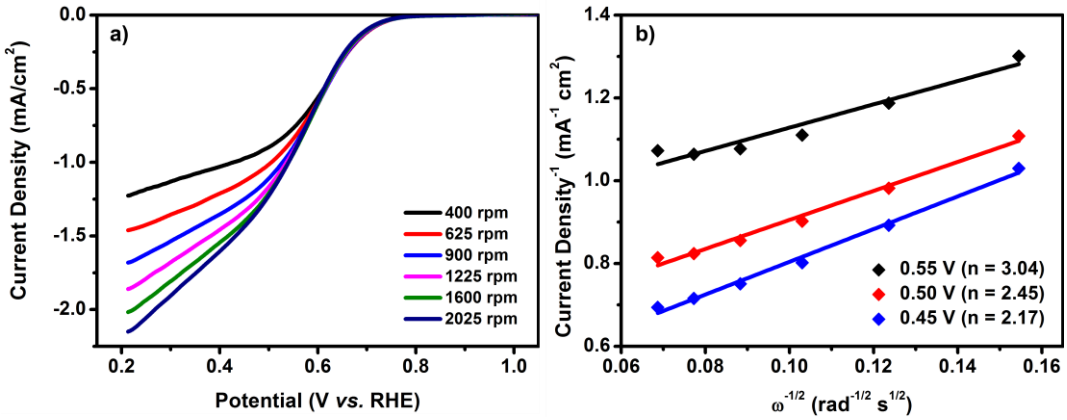

Fig. S16 a) LSV polarization curves of C_{700} in 0.1 M KOH at various rotating speeds. b) K–L plots of C_{700} at various potentials.

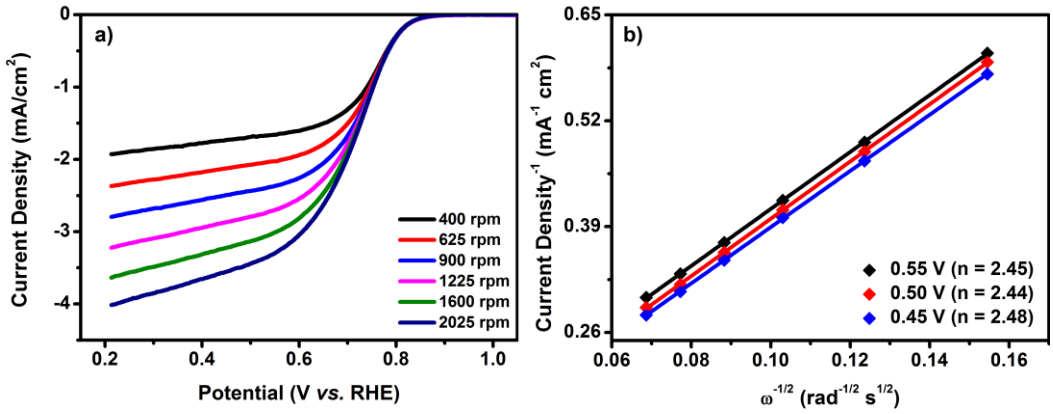

Fig. S17 a) LSV polarization curves of C_{800} in 0.1 M KOH at various rotating speeds. b) K–L plots of C_{800} at various potentials.

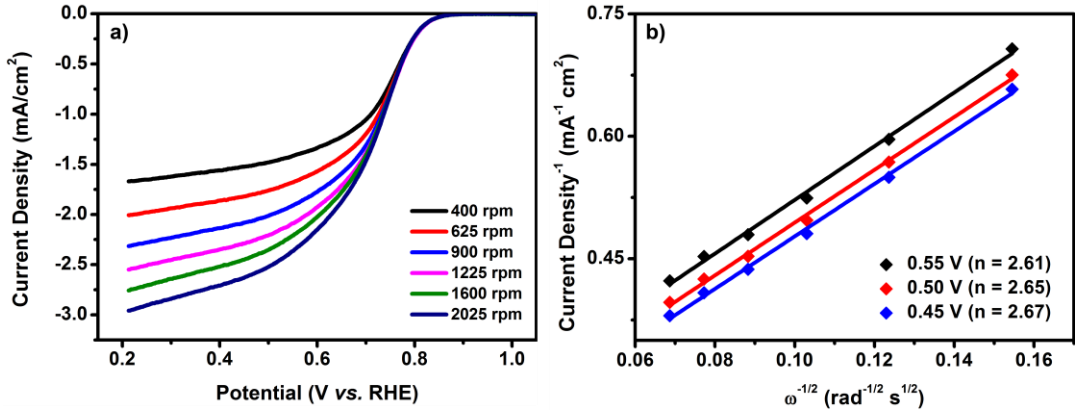

Fig. S18 a) LSV polarization curves of C_{900} in 0.1 M KOH at various rotating speeds. b) K–L plots of C_{900} at various potentials.

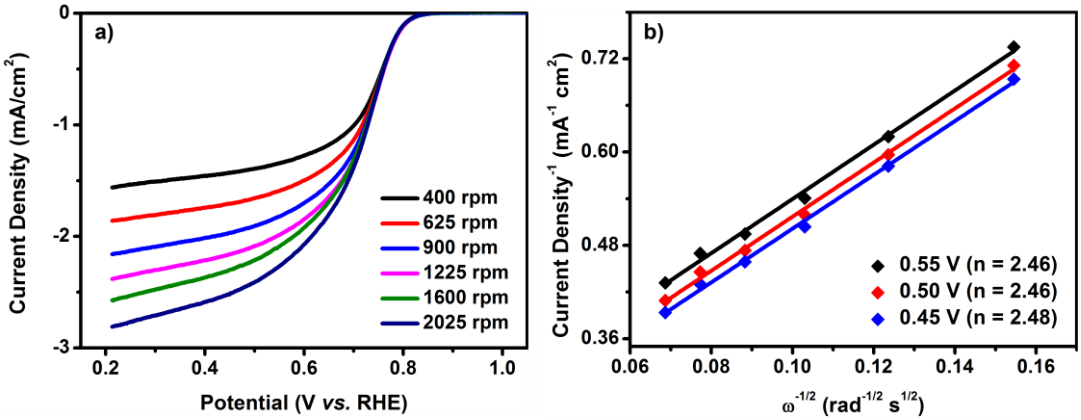

Fig. S19 a) LSV polarization curves of C_{1000} in 0.1 M KOH at various rotating speeds. b) K–L plots of C_{1000} at various potentials.